THE JOURNAL OF BIOLOGICAL CHEMISTRY
Vol. 275, No. 23, Issue of June 9, pp. 17297–17305, 2000

Printed in U.S.A.

Isohemoglobin Differentiation in the Bimodal-breathing Amazon Catfish *Hoplosternum littorale**

Received for publication, February 10, 2000, and in revised form, March 23, 2000
Published, JBC Papers in Press, March 27, 2000, DOI 10.1074/jbc.M001209200

Roy E. Weber‡§, Angela Fago‡¶, Adalberto L. Val‖, Anny Bang‡, Marie-Louise Van Hauwaert, Sylvia Dewilde¶**, Franck Zal**‡‡, and Luc Moens****

*From the ‡Department of Zoophysiology, University of Aarhus, DK 8000 Aarhus C, Denmark, the ‖Instituto Nacional de Pesquisas da Amazonia, Laboratory of Ecophysiology and Molecular Evolution, Alameda Cosme Ferreira 1756, 69083 Manaus, AM, Brazil, the **Biochemistry Department, University of Antwerp, Universiteitsplein 1, B-2610 Antwerpen, Belgium, and the ‡‡Equipe Ecophysiologie, Station Biologique de Roscoff, CNRS-UPMC-INSU, Place G. Teissier, B.P. 74 29682 Roscoff Cedex, France*

The bimodal gill(water)/gut(air)-breathing Amazonian catfish *Hoplosternum littorale* that frequents hypoxic habitats uses "mammalian" 2,3-diphosphoglycerate (DPG) in addition to "piscine" ATP and GTP as erythrocytic O_2 affinity modulators. Its electrophoretically distinct anodic and cathodic hemoglobins (Hb^{An} and Hb^{Ca}) were isolated for functional and molecular characterization. In contrast to Hb^{An}, phosphate-free Hb^{Ca} exhibits a pronounced reverse Bohr effect (increased O_2 affinity with decreasing pH) that is obliterated by ATP, and opposite pH dependences of K_T (O_2 association constant of low affinity, tense state) and the overall heat of oxygenation. Dose-response curves indicate small chloride effects and pronounced and differentiated phosphate effects, DPG < ATP < GTP < IHP. Hb^{Ca}-O_2 equilibria analyzed in terms of the Monod-Wyman-Changeux model show that small T state bond energy differences underlie the differentiated phosphate effects. Synthetic peptides, corresponding to N-terminal fragment of the cytoplasmic domain of trout band 3 protein, undergo oxygenation-linked binding to Hb^{Ca}, suggesting a metabolic regulatory role for this hemoglobin. The amino acid sequences for the α and β chains of Hb^{Ca} obtained by Edman degradation and cDNA sequencing show unusual substitutions at the phosphate-binding site that are discussed in terms of its reverse Bohr effect and anion sensitivities.

The ability of fish to colonize a large variation of biotopes is integrally related with the striking molecular and functional differentiation encountered in their hemoglobin (Hb)[1] systems. Variations in the functional properties of Hb result partly from variations in molecular structure that determine the intrinsic O_2 binding properties (1) and partly from regulatory changes in the physicochemical conditions under which they operate *in vivo*, such as red cell pH (that varies with ventilation rate and catecholamine stimulation) and in the type and concentration of heterotropic effectors like organic phosphates that decrease Hb-O_2 affinity (2–6).

In addition to "anodic" Hbs (Hb^{An}) that migrate anodically under normal electrophoretic conditions (pH ~8.6) and have relatively low O_2 affinities and marked Bohr effects (decreased O_2 affinity that enhances O_2 release in the acid tissues) and Root effects (reduction in O_2 binding capacity upon acidification that induces O_2 unloading in the swim bladder and retina), many fish species express "cathodic Hbs" (Hb^{Ca}) that have high isoelectric points and lack significant pH effects suggesting that they safeguard O_2 transport to tissues under hypoxic and acidotic conditions (7–9). Previous studies on the physiological and molecular implications of Hb multiplicity in fish have been concentrated on only a few species, such as rainbow trout, *Onchorhynchus mykiss,* and the eel *Anguilla anguilla* that exhibit radical differences, indicating the existence of diverse molecular strategies among teleosts. Thus, whereas cathodic HbI of trout lacks a Bohr effect and is insensitive to phosphate effectors (10, 11), cathodic eel Hb^{Ca} shows a reverse Bohr effect in the absence of phosphates and greater phosphate sensitivity than anodic eel Hb^{An} (12–14). Also, whereas the NTP pool of trout erythrocytes almost entirely consists of ATP, GTP is the main effector in eels, where it shows a greater effect on Hb-O_2 affinity and greater decreases in concentration following hypoxic exposure than ATP (12).

Deoxygenated Hb may also bind the cytoplasmic domain of erythrocytic band 3 proteins (cd-B3) in competition with glycolytic enzymes, as demonstrated for the human proteins (15, 16). The absence of effects of peptides corresponding to N-terminal fragments of trout cd-B3 on O_2 affinity of anodic trout HbIV, despite pronounced effects on human Hb (17), calls for closer study of Hb-band 3 interaction in fish.

Hoplosternum littorale, a small, heavily armored catfish from the Amazon basin, is an ideal model for investigating molecular adaptations in Hb function to extreme environmental conditions, bimodal breathing and modes of life. While using gills for gas exchange in well aerated water, it surfaces to swallow air in O_2-deficient waters and has a thin-walled part of the intestine

* This work was supported by the Danish Natural Science Research Council, the Danish Centre for Respiratory Adaptation, and the Fund for Scientific Research Projects G.2023.94 and G.0314.00, Flanders, Belgium. The costs of publication of this article were defrayed in part by the payment of page charges. This article must therefore be hereby marked "*advertisement*" in accordance with 18 U.S.C. Section 1734 solely to indicate this fact.

The sequences reported in this paper have been submitted to the Swiss Protein Database under Swiss-Prot accession numbers P82315 and P82316.

§ To whom correspondence should be addressed. Tel.: 45 8942 2599; Fax: 45 8619 4186; E-mail: roy.weber@biology.au.dk.

¶ Postdoctoral fellows of the Danish Centre for Respiratory Adaptation and the Belgian Fund for Scientific Research, respectively.

[1] The abbreviations used are: Hb, hemoglobin; Hb^{An}, electrophoretically anodic Hb; Hb^{Ca}, cathodic Hb; DPG, 2,3-diphosphoglycerate; cd-B3, cytoplasmic domain of Band 3 protein; MWC, Monod, Wyman and Changeux; K_T and K_R, O_2 association constant of low affinity, tense, and high affinity relaxed states, respectively, of Hb; RP-HPLC, reverse-phase-high performance liquid chromatography; BisTris, 2-[bis(2-hydroxyethyl)amino]-2-(hydroxymethyl)propane-1,3-diol; MES, 4-morpholineethanesulfonic acid.

that is kept devoid of food and appears to be a site for aerial gas exchange (18). The fish constructs floating nests of dead weed that expose the developing embryos to higher O_2 tensions than those prevailing in the water (18). A further peculiarity is that its red cells contain the "mammalian" cofactor DPG as well as "piscine" effectors ATP and GTP in approximately equal concentrations and that the DPG levels vary with environmental temperature (19, 20). It has single anodic and cathodic Hbs (that exhibits and lacks a Root effect, respectively) and shows no evidence for polymorphism in Hb multiplicity (21).

We report on the interactive effects of pH, the naturally occurring effectors ATP, GTP, DPG, and Cl^- and of IHP on O_2 binding of *Hoplosternum* Hb^{An} and Hb^{Ca}, and on the oxygenation-linked interaction with a synthetic peptide corresponding to the N terminus of trout cd-B3. In order to understand the structural and allosteric basis for its distinctive functional characteristics, we also analyzed the O_2 equilibria of Hb^{Ca} in terms of the two-state model for allosteric transitions (22), and we determined the primary structures of its globin chains.

EXPERIMENTAL PROCEDURES

Adult *H. littorale* (65) (14–16 cm, 45–66 × g) locally known as tamoata were collected by throw net in the Solimoes river near Marchantaria, Brazil. Blood was taken in heparinized syringes from the caudal blood vessels. Saline-washed red cells were frozen at −80 °C until use.

Hb was prepared as described previously (23) and dialyzed against 0.02 M Tris-HCl buffer, pH 8.4 (at 5 °C). Electrophoresis on cellulose acetate strips revealed only two Hb components that were separated by anion exchange chromatography on a 27 × 2 cm DEAE-Sephacel column equilibrated with the dialysis buffer and eluted in a 0–0.1 M NaCl gradient. Separated fractions were dialyzed for 24 h against three changes of CO-equilibrated 0.01 M HEPES, pH 7.7, containing $5{\cdot}10^{-4}$ M EDTA. All preparative steps were carried out at 0–5 °C. The Hb was frozen at −80 °C in 90–150-μl aliquots that were individually thawed immediately before experimentation. Stripped human Hb for control measurements was prepared as described previously (24) from blood of a non-smoking adult.

O_2 Binding—O_2 binding equilibria were measured using a modified diffusion chamber, where ultrathin layers of Hb solution were equilibrated with pure (>99.998%) N_2 or O_2 or stepped mixes of these and air prepared with Wösthoff pumps to ensure full equilibration at each step (23, 25). The pH of Hb solutions was adjusted using HEPES buffers for pH ~6.5–8.2, MES buffers for lower, and glycine buffer for higher pH values (final buffer concentration, 0.10 M). The pH was measured in oxygenated (air-equilibrated) Hb samples using a BMS2 Mk2 Blood Micro system and PHM 64 Research pH meter (Radiometer, Copenhagen, Denmark). Chloride was added as KCl and measured using a Radiometer CMT10 chloride titrator. ATP, GTP, and DPG concentrations in stock samples were assayed using Sigma test chemicals. The effects of anions on O_2 equilibria were measured at pH near 7.5 and 7.0, whereafter the P_{50} (half-saturation O_2 tension) and n_{50} (Hill cooperativity coefficient at P_{50}) values at these exact pH values were interpolated from linear regressions. The overall heat of oxygenation $\Delta H'$, which includes the heat of solution of O_2 (-13 kJ·mole^{-1}) and the heats of processes linked to O_2 binding such as proton and anion dissociation, was evaluated as $R{\cdot}(\Delta \ln P_{50})/\Delta(1/T)$, where R is the gas constant. The effects of synthetic peptides corresponding to the first 10 and 20 amino acid residues of trout cd-B3 on Hb-O_2 affinity was examined as earlier described (17). The sequence of the 20-mer peptide is Met-Glu-Asn-Asp-Leu-Ser-Phe-Gly-Glu-Asp-Val-Met-Ser-Tyr-Glu-Glu-Glu-Ser-Asp-Ser (the 10-mer comprises the first 10 residues) (26).

To analyze the allosteric interactions, precise O_2 equilibria measured with focus on extreme (low and high) saturation values were analyzed in terms of the MWC model (22), evaluating K_T and K_R, the allosteric constant (L), and derived parameters, including q, ΔG, P_m, and n_{max} (where q is the number of interacting O_2-binding sites; ΔG is the free energy of cooperativity; P_m is the median O_2 tension; and n_{max} is the maximum cooperativity) (see Table I) as described by Weber *et al.* (27).

Reverse-phase Chromatography—Heme was removed from purified Hb^{Ca} by acid-acetone precipitation (28). Globin chains were reduced for 5 min at 100 °C in 50 mM Tris-HCl, pH 7.0, 6 M guanidinium chloride, 1% 2-mercaptoethanol and modified with 4-vinylpyridine and maleic anhydride as described previously (29). Samples were acidified with trifluoroacetic acid and applied to a Prosphere RP C_4 5-μm column (300 Å; 4.6 × 250 mm; Alltech Associates, Inc.) equilibrated with 5% acetonitrile in 0.1% aqueous trifluoroacetic acid. The samples were eluted with a linear gradient of 5–75% acetonitrile in 0.1% trifluoroacetic acid over 45 min at a flow rate of 1 ml/min. Absorbance of the eluate was monitored at 280 nm.

Enzymatic Digestion and Peptide Isolation—Globin chains were digested with trypsin at an enzyme:substrate ratio of 1:50 in 200 mM NH_4HCO_3, pH 8.3, at 37 °C for 6 h. The digested products were isolated by RP-HPLC as described for the globin chain isolation. The amino acid sequence of peptides was determined with an automated protein sequencer ABI 471 B (Applied Biosystems), according to the manufacturer's recommendations.

Primer Design and cDNA Sequencing—By using the amino acid sequence of the β chain, the degenerated primer HOPLO F1, TGGGGNAARATHCAYATHGA, a 20-mer with 144 redundancies, was designed corresponding to the sense strand predicted by the peptide

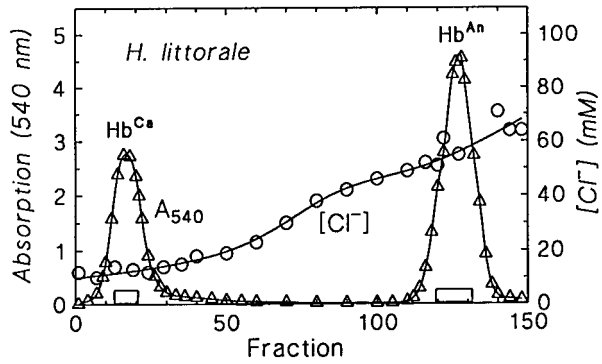

FIG. 1. **Separation of cathodic Hb^{Ca} and anodic Hb^{An} of *Hoplosternum littorale* by DEAE-ion exchange chromatography.** Δ, absorption at 540 nm; ○, chloride concentration; *rectangles*, fractions pooled for functional and structural characterization.

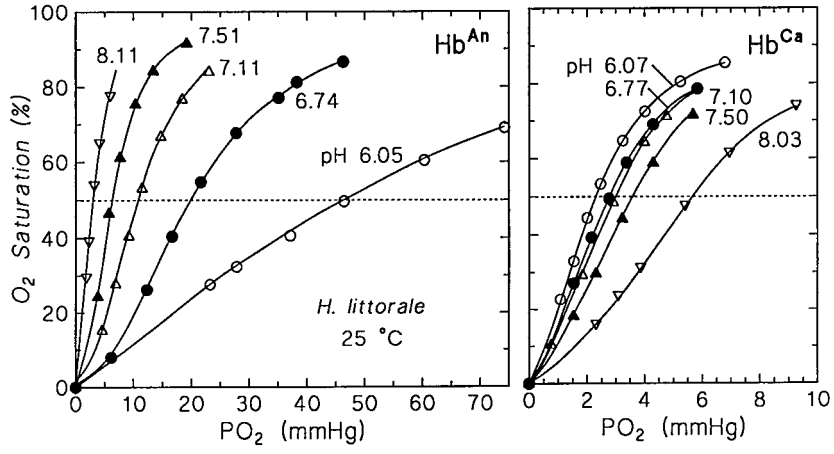

FIG. 2. **O_2-binding curves of *Hoplosternum* Hb^{An} and Hb^{Ca}, measured in 0.1 M HEPES buffer at 25 °C, showing opposite Bohr effects.** Heme concentration, 0.15 mM (Hb^{An}) and 0.14 mM (Hb^{Ca}).

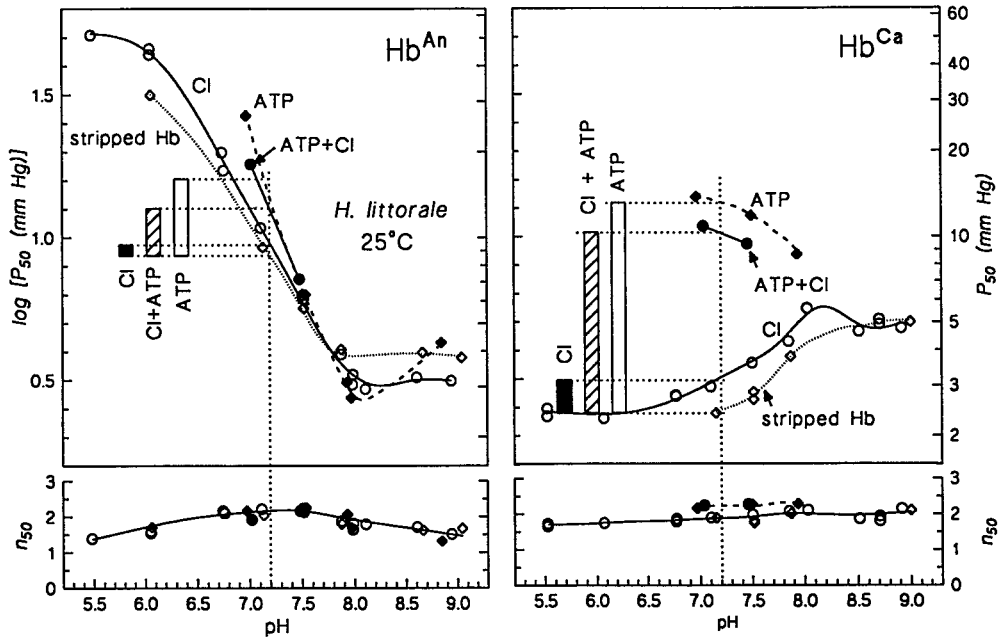

FIG. 3. **P_{50} and n_{50} values of *Hoplosternum* Hb^{An} and Hb^{Ca} at 25 °C and their pH dependence in the absence (*diamonds*) and presence (*circles*) of chloride and the absence (*open symbols*) and presence (*solid symbols*) of saturating ATP concentrations (ATP:Hb_4 ratio ≥100).** As shown ATP and chloride enhance the normal Bohr effect in Hb^{An} and reverse the Bohr effect in Hb^{Ca}. Histograms show $\Delta\log P_{50}$ values induced at pH 7.2 by 0.10 M chloride (*solid columns*), ATP (*open columns*), and 0.10 M chloride and ATP (*obliquely hatched columns*). Other conditions as in Fig. 2.

fragment WGKIHID (Fig. 10). Total RNA was isolated from intact erythrocytes with a micro RNA isolation kit (Stratagene). First strand cDNA was synthesized with MMLV-RT (Promega) using an oligo(dT) primer. PCR reactions were carried out using HOPLO F1 and oligo(dT). The PCRs were carried out for 30 cycles of 94 °C for 30 s, 50 °C for 1.0 min, and 72 °C for 1.5 min with *Taq* polymerase on a GeneAmp PCR system 9600 (Perkin-Elmer). Sequencing was then performed with HOPLO F1 as primer on an ABI 377 automatic sequencer (Applied Biosystems, Inc.) according to the manufacturer's recommendations.

Electrospray Ionization Mass Spectrometry—Electrospray data were acquired on a Quattro II triple quadrupole mass spectrometer (Micromass Ltd.) as described elsewhere (30).

RESULTS

Oxygenation Studies—Anion exchange chromatography resolves the Hb into two distinct fractions, Hb^{Ca} and Hb^{An}, occurring in a ratio of approximately 38:62 (Fig. 1). The oxygenation characteristics of Hb^{An} and Hb^{Ca} are radically different. At pH 7.2, the approximate intracellular value, the affinity of stripped Hb^{Ca} markedly exceeds that of Hb^{An} (P_{50} = 2.4 and 8.7 mm Hg, respectively, at 25 °C) (Figs. 2 and 3). In contrast to the pronounced normal Bohr effect in Hb^{An} ($\varphi = \Delta\log P_{50}/\Delta pH = -0.56$ at pH 7.2), Hb^{Ca} exhibits a marked, reverse Bohr effect ($\varphi = +0.38$). Due to opposite pH effects the functional differentiation between the two isoHbs increases with falling pH.

Hb^{Ca} exhibits much greater sensitivity to ATP than Hb^{An}. The phosphate effects increase with falling pH, whereby the presence of ATP induces a slight normal Bohr effect in Hb^{Ca} ($\varphi = -0.14$ at pH 7.2) and almost obliterates the affinity difference between the two Hb components (Fig. 3). Significantly, ATP alone decreases O_2 affinity of both components more than ATP in the presence of 100 mM Cl^- (as illustrated for pH 7.2 by the $\Delta\log P_{50}$ columns in Fig. 3). The Hill coefficient n_{50} approximates 2.0 in both Hbs at pH 6.5–8.0, decreases at low and high pH to 1.5 in Hb^{An}, and at low pH to 1.7 in Hb^{Ca} (Fig. 3) but increases to 2.4 in Hb^{Ca} in the presence of ATP.

The difference between the Bohr effect curves at 10 and 25 °C (Fig. 4) illustrates a large overall temperature effect ($\Delta H'$ about −85 kJ·mol^{-1}) in Hb^{An} at high pH (8.7) where the Bohr effect and phosphate binding disappear (*cf.* Fig. 3). At lower

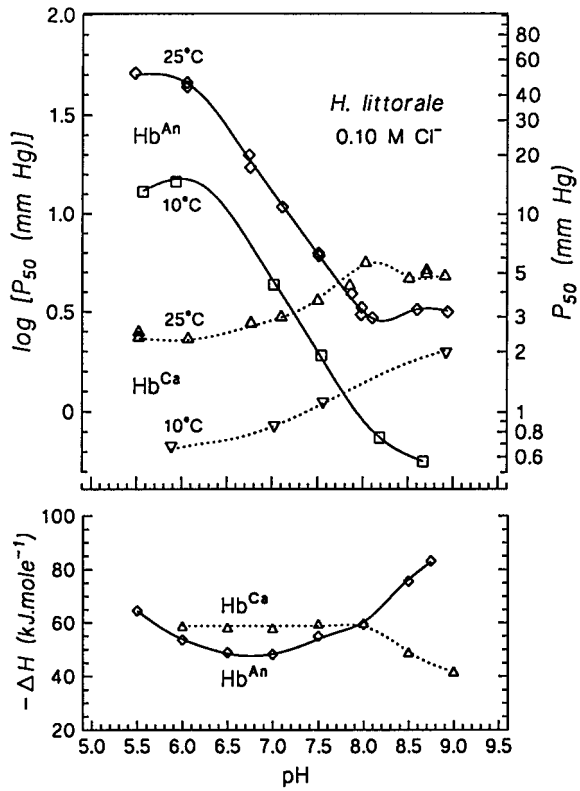

FIG. 4. **Bohr effects ($\Delta\log P_{50}/\Delta pH$) of *Hoplosternum* Hb^{An} (□, ◇) and Hb^{Ca} (▽, △) at 10 (▽, □) and 25 °C (△, ◇) (*upper panel*), and the pH dependence of the overall heat of oxygenation ($\Delta H'$) (*lower panel*) measured in the presence of 0.10 M KCl.** Heme concentration, 0.14 mM.

pH, where the Bohr effect is operative, the enthalpy of oxygenation decreases to approximately −45 kJ·mol^{-1} at pH 6.8 reflecting endothermic proton release. Given that the Bohr factor (0.65) gives the moles of protons dissociated per mol of O_2

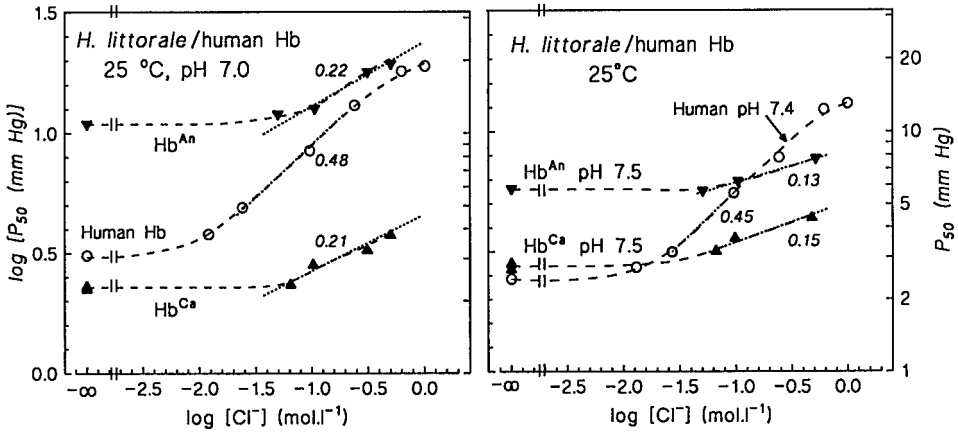

FIG. 5. **Effects of chloride concentration on P_{50} of *Hoplosternum* Hb^{An} (▼) and Hb^{Ca} (▲) at pH 7.0 (*left panel*) and pH 7.5 (*right panel*), compared with effects on human Hb (○, after Ref. 24) at pH 7.0 (*left panel*) and 7.4 (*right panel*).** Heme concentration, 0.6 mM.

bound, the enthalpy difference (+40 kJ·mol of heme) indicates an apparent heat of proton dissociation of 62 kJ·mol^{-1}. Analogously the increase in enthalpy for Hb^{Ca} (by approximately 18 kJ·mol^{-1} as pH decreases from pH 9, Fig. 4) reflects proton association upon O_2 binding, in accordance with the reverse Bohr effect. Related to the Bohr factor (+0.38) this increase indicates an apparent ionization enthalpy of approximately 47 kJ per mol of protons bound. These values may, however, be biased by thermodynamic contributions from other oxygenation linked processes, such as Cl^- binding, that may account for the lower ΔH value found in Hb^{An} at pH 6.0 than at pH 8.5 (where oxygen-linked proton binding approximates zero).

Chloride ions reduce O_2 affinity of both Hb^{An} and Hb^{Ca}, except for HbA at pH >7.7 where 0.1 M chloride increased affinity (Fig. 3). Below pH 7.7 chloride and saturating ATP concentration raise the Bohr effect of Hb^{An} to −0.65 and −1.1, respectively. The chloride sensitivity of *Hoplosternum* Hbs is low compared with human Hb. At pH 7.0, 100 mM chloride increases log P_{50} of Hb^{An} and Hb^{Ca} by only 0.07 units, compared with 0.45 units in human Hb (Figs. 3 and 5).

Dose-response curves for the effects of anions (A) on O_2 affinity (Figs. 5 and 6) can be interpreted in terms of the basic linkage equation: $\Delta\log P_m/\Delta\log[A] = -\Delta X$, where X is the amount of anion bound per (de-)oxygenated heme. Provided close agreement exists between P_{50} and P_m values (see below) and between the concentration and activity of the effector, the slopes of log P_{50} *versus* log[A] plots at midpoint (designated by τ) approach a limiting value that cannot be smaller than the number of oxygen-linked binding sites per heme (24, 31).

The log P_{50} *versus* log[Cl^-] curves indicate τ values of approximately 0.22 for *Hoplosternum* Hb^{An} and Hb^{Ca} compared with 0.48 for human Hb at pH 7.0 and lower values at higher pH (τ = 0.13–0.14 for *Hoplosternum* Hbs at pH 7.5 and 0.45 for human Hb at pH 7.4) (Fig. 5).

Dose-response curves for the phosphate effectors (Fig. 6) reveal the order of allosteric effectivity as DPG < ATP < GTP < IHP, greater sensitivities of Hb^{Ca} than Hb^{An} to all effectors and greater effects at pH 7.0 than at pH 7.5, where the cationic phosphate-binding sites are less charged. Curiously, DPG and low concentrations of the other effectors increased O_2 affinity of Hb^{An} at pH 7.5 (Fig. 6*D*).

For Hb^{Ca} the curves at pH 7.0 and 7.5 (Fig. 6, *A* and *B*) indicate lower maximum P_{50} values induced by DPG than by IHP, ATP, and GTP, indicating formation of additional bonds (*cf.* Ref. 32) with the latter effectors at saturating phosphate:Hb ratios. Whereas the slope for DPG and Hb^{Ca} (τ = 0.22) tallies with the release of one phosphate molecule per oxygenated tetramer, higher τ values (>0.25) obtained for ATP, GTP, and IHP suggest the existence of additional sites of phosphate interaction.

Interpolated on the basis of the P_{50} maximum induced by IHP (Fig. 6*A*), the data indicate apparent dissociation equilibrium constants, K_a (estimated as the effector concentration that induces half of the maximum change in log P_{50}) for the reactions of Hb^{Ca} with ATP, GTP, and IHP at pH 7.0 of approximately 11×10^{-4}, 5.4×10^{-4}, and 2.2×10^{-4} M, respectively. Interpolated in terms of the P_{50} maximum induced by DPG, the constant for DPG approximates 13.2×10^{-4} M. Compared with values for the reaction of DPG with human and Eskimo dog Hbs (3.2×10^{-4} M at pH 7.5 and ~1×10^{-4} M at pH 7.2, respectively, at 20 °C and in the presence of 100 mM Cl^-) (33, 34), this illustrates relatively low DPG sensitivity in *Hoplosternum* Hb^{Ca}.

In contrast to the pronounced effects of the 10- and 20-mer synthetic trout band 3 peptides on the O_2 affinity of human Hb (Fig. 7; see also Ref. 17), the peptides had no effect on *Hoplosternum* Hb^{An} at pH 7.2 and only marginally decreased the O_2 affinity at lower pH (6.4) (Fig. 7). This aligns with the absence of effects in trout Hbs I-IV (17),[2] despite the large effects of these peptides in human Hb (17). Significantly, the peptide exerts a distinct effect on *Hoplosternum* Hb^{Ca} at pH 7.2 and an even greater effect at lower pH (6.58) (Fig. 7). The effect on human Hb (17) and the marked pH-dependent effects in *Hoplosternum* Hb^{Ca} (Fig. 7) attest to the functionality of the peptides and the presence of a putative band 3-binding site in both Hbs.

The allosteric and derived MWC model parameters are given in Table I. The agreement between n_{50} and n_{max} and between P_{50} and P_m values reflects highly symmetrical O_2 equilibrium curves that permit rigorous analysis of P_{50} plots. Moreover, the mean value for the number of interacting O_2-binding sites per molecule (q = 4.03 ± 0.74), obtained when q was fit along with the other parameters to obtain the best possible fit in the 13 condition sets described in Table I, tallies neatly with a tetrameric structure. The derived parameters summarized in Table I were thus obtained with q fixed at 4.

Extended Hill plots for the effects of pH and organic phosphates in Hb^{Ca} are shown (Figs. 8 and 9). In contrast to anodic vertebrate Hbs where the normal alkaline Bohr effect primarily results from a decrease in K_T with increasing proton concentrations (23, 35, 36), the control mechanism of the reverse Bohr effect of *Hoplosternum* Hb^{Ca} is an *in*crease in K_T with falling pH (Fig. 8, Table I), indicating a more constrained T

[2] R. E. Weber, unpublished observations.

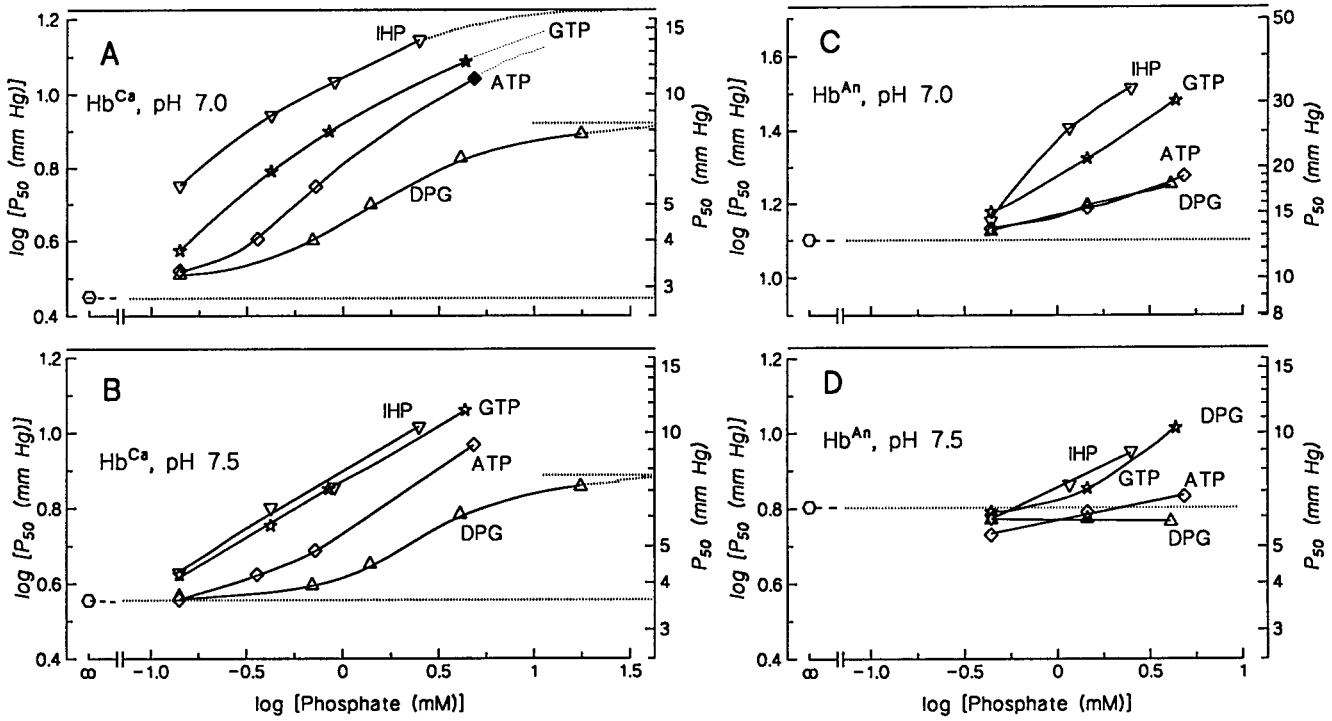

FIG. 6. **Effects of DPG, ATP, GTP, and IHP concentrations on P_{50} values of *Hoplosternum* Hb^{An} (*left panels*) and Hb^{Ca} (*right panels*) at pH 7.0 (*upper panels*) and pH 7.5 (*lower panels*), measured at 25 °C in the presence of 0.10 M KCl.** Heme concentrations, 0.14 (Hb^{Ca}) and 0.15 (Hb^{An}). ∞ indicates zero phosphate concentration.

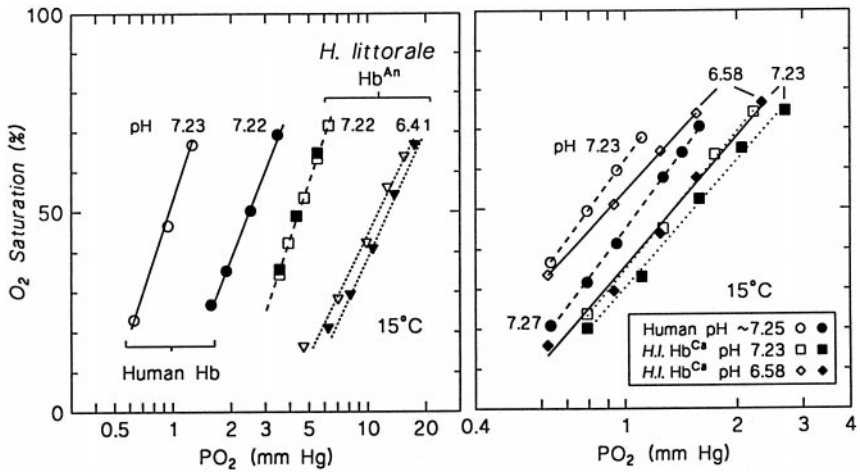

FIG. 7. **Semilogarithmic plots of O_2 equilibria of *Hoplosternum* and human Hbs in the absence (*open symbols*) and presence (*closed symbols*) of synthetic peptides corresponding to the N-terminal segment of the cytoplasmic fragment of band 3 protein (cd-B3) of rainbow trout at the indicated pH values.** Effects of 20-mer peptide on human Hb and *Hoplosternum* Hb^{An} (*left panel*) and of 10-mer peptide on *Hoplosternum* Hb^{Ca} (*right panel*). Heme concentration, 0.30 mM (*Hoplosternum* Hbs) and 0.63 mM (human Hb). Peptide: tetrameric Hb ratio, 5.

TABLE I

MWC and derived parameters for Hoplosternum Hb^{Ca} and their pH and cofactor sensitivities, derived for q = 4

pH	Cofactor:cofactor/Hb_4	P_{50}	n_{50}	n_{max}	P_m	K_T ± S.E.	K_R ± S.E.	L	ΔG
		mm Hg			*mm Hg*	*mm Hg^{-1}*	*mm Hg^{-1}*		*kJ·mol^{-1}*
7.082		2.86	2.02	2.03	2.73	0.122 ± 0.0096	2.000 ± 0.332	9.0×10^2	06.45
7.522		3.74	2.25	2.25	3.66	0.0663 ± 0.0043	1.459 ± 0.1127	8.2×10^2	07.43
7.677		4.27	2.17	2.18	4.09	0.0706 ± 0.0071	1.463 ± 0.2361	1.3×10^3	07.16
8.080		5.08	2.39	2.42	4.78	0.0551 ± 0.0054	2.039 ± 0.3753	9.1×10^3	08.54
7.517	ATP:2.6	5.82	2.41	2.42	5.67	0.0385 ± 0.0014	1.161 ± 0.0508	1.9×10^3	08.24
7.526	ATP:27.8	12.39	2.68	2.72	11.63	0.0185 ± 0.0015	1.405 ± 0.3574	7.2×10^4	10.37
7.506	ATP:32	15.99	2.69	2.70	15.42	0.0120 ± 0.00061	0.669 ± 0.0560	1.1×10^4	09.81
7.516	GTP:2.5	7.93	2.59	2.60	7.61	0.0272 ± 0.0012	1.272 ± 0.0768	8.8×10^3	09.32
7.525	GTP:28.8	15.85	2.75	2.79	14.94	0.0133 ± 0.00072	1.164 ± 0.1399	9.2×10^5	10.76
7.532	DPG:2.53	4.80	2.48	2.48	4.80	0.0368 ± 0.0026	1.196 ± 0.0602	1.1×10^3	08.49
7.512	DPG:27.9	8.22	2.52	2.53	7.90	0.0274 ± 0.0011	1.099 ± 0.0713	5.7×10^3	08.93
7.535	IHP:2.52	10.37	2.69	2.72	9.84	0.0205 ± 0.00093	1.354 ± 0.1144	3.2×10^4	10.13
7.580	IHP:27.7	17.64	2.75	2.80	16.58	0.0122 ± 0.00066	1.125 ± 0.1429	1.2×10^5	10.85

state with increasing pH. The Bohr factor of the deoxygenated (T state) Hb markedly exceeds that at median saturation (φ = +0.35 *versus* +0.25, respectively, at pH 7–8; Fig. 8, *inset*). Increased pH accordingly raises the free energy of cooperativity (ΔG increases from approximately 6.5 to 8.5 kJ·mol between pH 7 and 8, see Table I) as illustrated by the greater distance

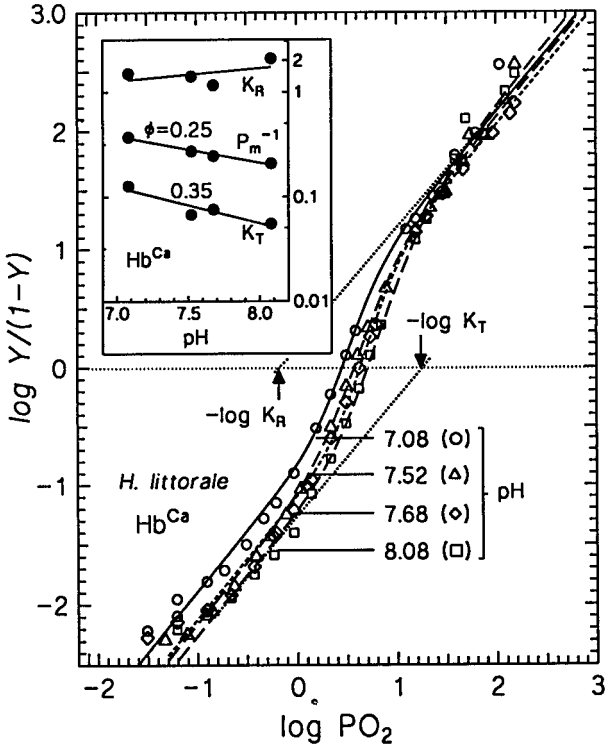

FIG. 8. **Extended Hill plots of stripped *Hoplosternum* Hb^{Ca} at 25 °C and the indicated pH values.** As shown, K_T and K_R values are evident from intersections of upper and lower asymptotes of slope unity with x axis at log $Y/(1 - Y) = 0$. *Inset,* pH dependence of K_T, $1/P_m$, and K_R values. Heme concentration, 0.64 mM.

between the upper and lower linear asymptotes of the extended Hill plots at high pH (see Fig. 8). The allosteric constant L of *Hoplosternum* Hb^{Ca} increases at high pH (Table I), compared with the opposite effect in human and anodic fish Hbs (23, 35).

In contrast to protons, ATP, GTP, DPG, and IHP modulate O_2 affinity of *Hoplosternum* Hb^{Ca} by decreasing K_T (Fig. 9) as in anodic mammalian and fish Hbs (23, 35, 37). The τ values for K_T, P_m, and K_R (deduced from the slopes of data sets in the *inset* of Fig. 9) reflect T state, median, and R state "DPG factors" of 0.33, 0.25, and 0.0. The lack of pronounced effects on K_R values in *Hoplosternum* Hb^{Ca} (Fig. 9, *inset*) differs from the reductions in K_R observed in the presence of high NTP:Hb_4 ratios in anodic tench Hb (23).

Structural Characterization—Separation of the α and β chains of the *Hoplosternum* Hb^{Ca} by RP-HPLC and their molecular masses determined by electrospray ionization mass spectrometry as 15,542.0 and 15,978.0, respectively, are shown in Fig. 10.

N-terminal sequencing showed that the α chain was blocked, whereas the β chain was directly accessible for Edman degradation, as commonly observed in teleost Hbs. The α chain was unblocked by heating at 55 °C in 30% trifluoroacetic acid for 3 h. The *S*-pyridylethylated and *S*-pyridylethylated/maleilated globin chains were digested with trypsin, and the resulting peptides were separated by RP-HPLC. All peaks were sequenced. Some peaks contained 2 or 3 peptides, but their sequences were deduced unambiguously by subtraction of peptides sequenced in other peaks.

The α and β chains of *Hoplosternum* Hb^{Ca} consist of 142 and 146 amino acid residues, respectively. Alignment of the globin chains with those for eel *A. anguilla* (13) Hb and rainbow trout *O. mykiss* (38) Hb is presented in Fig. 11. The sequences align well and without any ambiguity with other fish globin chains. In order to confirm the sequence showed in Fig. 11, we performed partial cDNA sequencing as described under "Experimental Procedures." The amino acid sequence thus deduced confirms the sequence obtained at the protein level.

The sequence-deduced molecular weights are 15,544.1 and 15,976.3 for the α and β chains, respectively. These values are in excellent agreement with the experimentally determined mass data (15,542.0 ± 2.0 and 15,978.0 ± 2.0 for the α and β chains, respectively) where the mass for the α chain is corrected for the N-terminal acetylation.

Remarkably, position NA2(2β) is occupied by His, as in mammals, in contrast to other teleosts that have Glu or Asp (exceptionally Lys) (39) at this phosphate-binding site. Similarly notable is the presence of Ser at H-21(β143), compared with His in mammals and Lys or Arg in other fish (except trout HbI that has Ser and lacks phosphate sensitivity).

DISCUSSION

The marked functional differentiation between *Hoplosternum* Hb^{An} and Hb^{Ca} agrees with earlier findings of Garlick *et al.* (21). In contrast to their study carried out in the presence of ionic (Tris/BisTris) buffers that may perturb the Bohr and phosphate effects due to higher chloride levels at low pH values (24), the present work carried out using zwitterionic HEPES buffer shows much lower Bohr factors ($\varphi = -0.56$ compared with -0.98 for Hb^{An}).

The Reverse Bohr Effect—What may be the significance of a reverse Bohr effect in Hb^{Ca} that is obliterated by ATP? In view of the greater reduction of O_2 affinity by phosphates at low pH, we propose that a reverse Bohr effect in phosphate-free solution is a precondition for small *in vivo* pH effects associated with pronounced phosphate sensitivity.

Apart from *Hoplosternum*, Hbs with pronounced reverse Bohr effects occur in the facultative air-breathing teleost *Pterygoplichthys pardalis* (21, 40), the surface skimmer *Mylossoma* sp. (41), frog tadpoles, and aquatic salamanders (*cf.* Ref. 13) suggesting implication in the utilization of alternative sources of O_2. The reverse Bohr effect and strong phosphate sensitivity in *Hoplosternum* Hb^{Ca} contrast with lack of Bohr and NTP effects in cathodic trout HbI but accord with data for eel *Anguilla* (12–14), *Mylossoma* (41), and *Pterygoplichtys* (40), indicating that the intensively studied trout HbI is an exceptional rather than prototype cathodic Hb.

In human Hb, the main Bohr groups are N-terminal Val-NA1(α1) and the C-terminal His-HC3(β146) that account for about 30 and 50–65%, respectively, of the normal Bohr effect, whereas His-H21(β143) is considered to be involved in the expression of the reverse ("acid") Bohr effect that reflects the uptake of protons upon oxygenation at low pH (<6.5) (42–44). With Val-NA1 acetylated in fish Hbs, the absence of a normal Bohr effect in stripped *Hoplosternum* Hb^{Ca} correlates with the His → Phe-HC3(β146) replacement, as found in cathodic Hbs of trout, eel, and catfish (7, 13, 38). The reverse Bohr effect becomes apparent only when the major alkaline Bohr groups are replaced (as in cathodic Hbs) or inoperative (as in anodic Hbs that exhibit reverse Bohr effects at high pH) (13, 45). Apart from the HC3(β146) substitution, *Hoplosternum* Hb^{Ca} shows a His → Asn-FG4(β94) replacement that also is encountered in eel Hb^{Ca} and other reverse Bohr effect Hbs, providing further evidence for involvement of His-FG4(β94) in the alkaline Bohr effect of fish Hbs (45). Interestingly, Ser-F9(β93), which typically is conserved in fish Hbs with normal Bohr and Root effects and which has been considered to donate a hydrogen bond to His-HC3(β146) (46), is substituted by Cys in *Hoplosternum* Hb^{Ca} and by Asn in eel Hb^{Ca}. Cys at F9(β93) is another mammalian trait and highly exceptional in fish Hbs.

The molecular mechanism proposed for the reverse Bohr effect in eel Hb^{Ca} (13) visualizes the implication of the residues

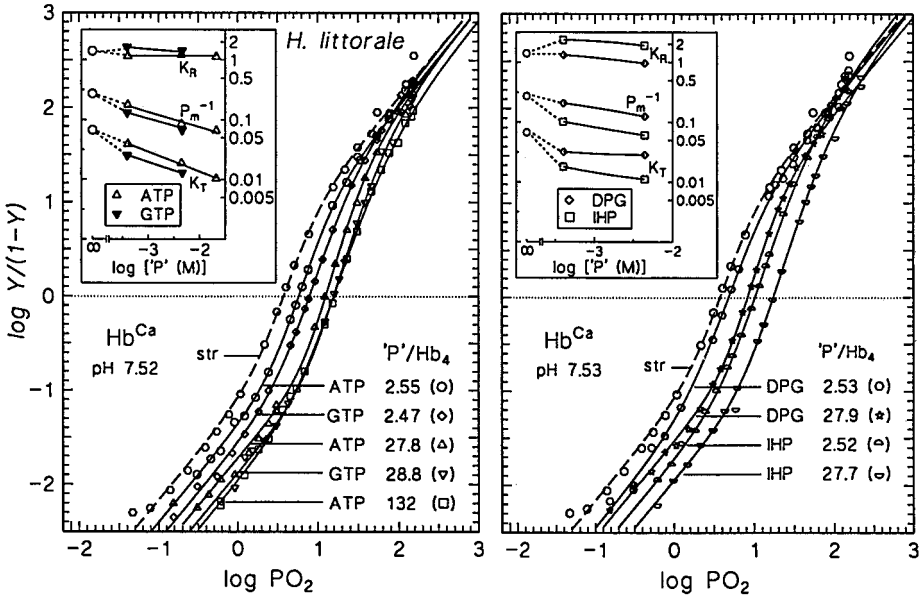

FIG. 9. **Extended Hill plots of stripped *Hoplosternum* Hb^{Ca} at 25 °C and pH 7.5 in the absence of phosphates (*str*) and in the presence of ATP and GTP (*left panel*) and DPG and IHP (*right panel*) at the indicated phosphate to Hb(tetramer) ratios.** *Insets,* dependence of log(K_T, $1/P_m$, and K_R (mm Hg^{-1})) on log[phosphate]. Heme concentration, 0.64 mM.

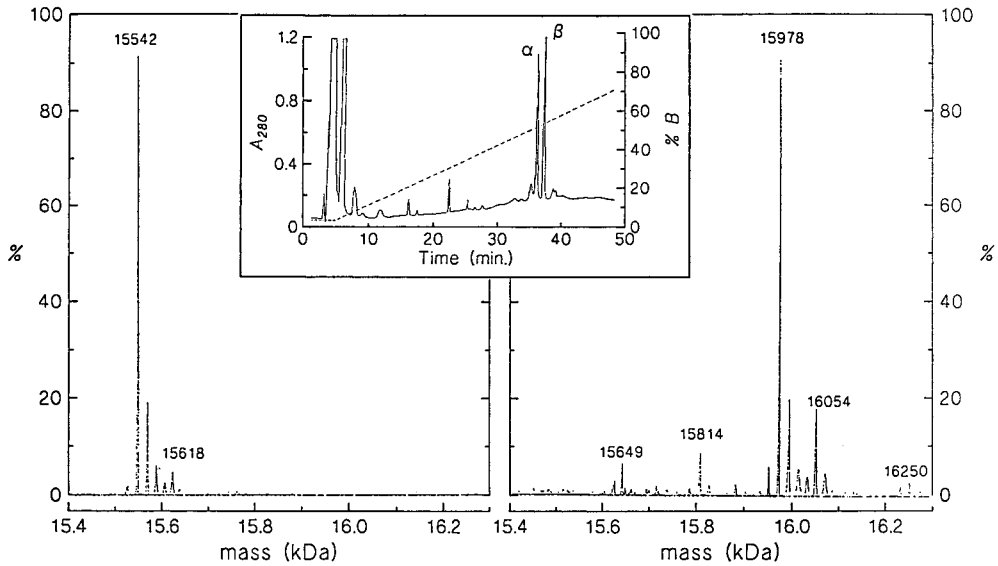

FIG. 10. **Separation of globin chains of *Hoplosternum* Hb^{Ca} by RP-HPLC (*inset*) and the electrospray mass spectrum obtained for the α chain (*left*) and β chain (*right*).**

at the phosphate-binding site that in fish Hbs include Val-NA1(β1), Glu-NA2(β2), Lys-EF6(β82), and Arg-H21(β143). In the T state the proximity of positively charged amino acid residues in the central cavity reduces their affinity for protons (whereas their pK_a values are normal in the R state), whereby the groups implicated in organic phosphate binding become reverse Bohr groups in the absence of phosphates. In other words, protons destabilize the T state, as is evident from the increase of K_T with pH decrease, whereas the O_2 affinity of the R state is practically unaffected (Fig. 8; Ref. 14). Accordingly, the reverse Bohr effect in *Hoplosternum* Hb^{Ca} having His at NA2(β2) is almost twice as large as that in eel Hb^{Ca} having Glu-NA2(β2) (φ = +0.38 and +0.2, respectively), indicating that more positively charged groups in the central cavity contribute to this effect in *Hoplosternum*.

To our knowledge the increase in overall oxygenation enthalpy of Hb^{Ca} (increased temperature sensitivity) with falling pH (Fig. 4) provides the first demonstration of the thermodynamic consequences of O_2-linked proton binding associated with a reverse Bohr effect. The opposite pH dependence of the temperature effects in Hb^{An} and Hb^{Ca} (Fig. 4) would tend to keep a constant and pH-independent *in vivo* heat of oxygenation.

Organic Phosphate Interaction—Most fish Hbs have Glu at NA2(β2), which accepts hydrogen bonds from strain-free ATP and GTP molecules (47). The presence of His at NA2(β2) in *Hoplosternum* Hb^{Ca} is exceptional for teleosts and other ectothermic vertebrates, where its distribution suggests a correlation with air breathing or the presence of alternative red cell phosphates. As listed (48) it occurs in the Hbs of the lungfish *Lepidosiren paradoxa,* where 6–8% of its erythrocytic phosphates is inositol diphosphate (49), the sharks *Squalus acanthias* and *Heterodontus portusjacksoni,* where high erythrocytic urea levels antagonize the modulator effectivity of ATP (50), and tadpoles of the frog *Rana catesbeiana* and the toad *Xenopus laevis*. Alternatively, the episodic occurrence of His-NA2 in elasmobranchs, lungfish, and developmental stages of higher vertebrates suggests that it may be a phylogenetically primitive character that was deleted in most non-mammalian vertebrates.

The occurrence of high levels of DPG in *Hoplosternum* erythrocytes together with the "mammalian DPG-binding" residue

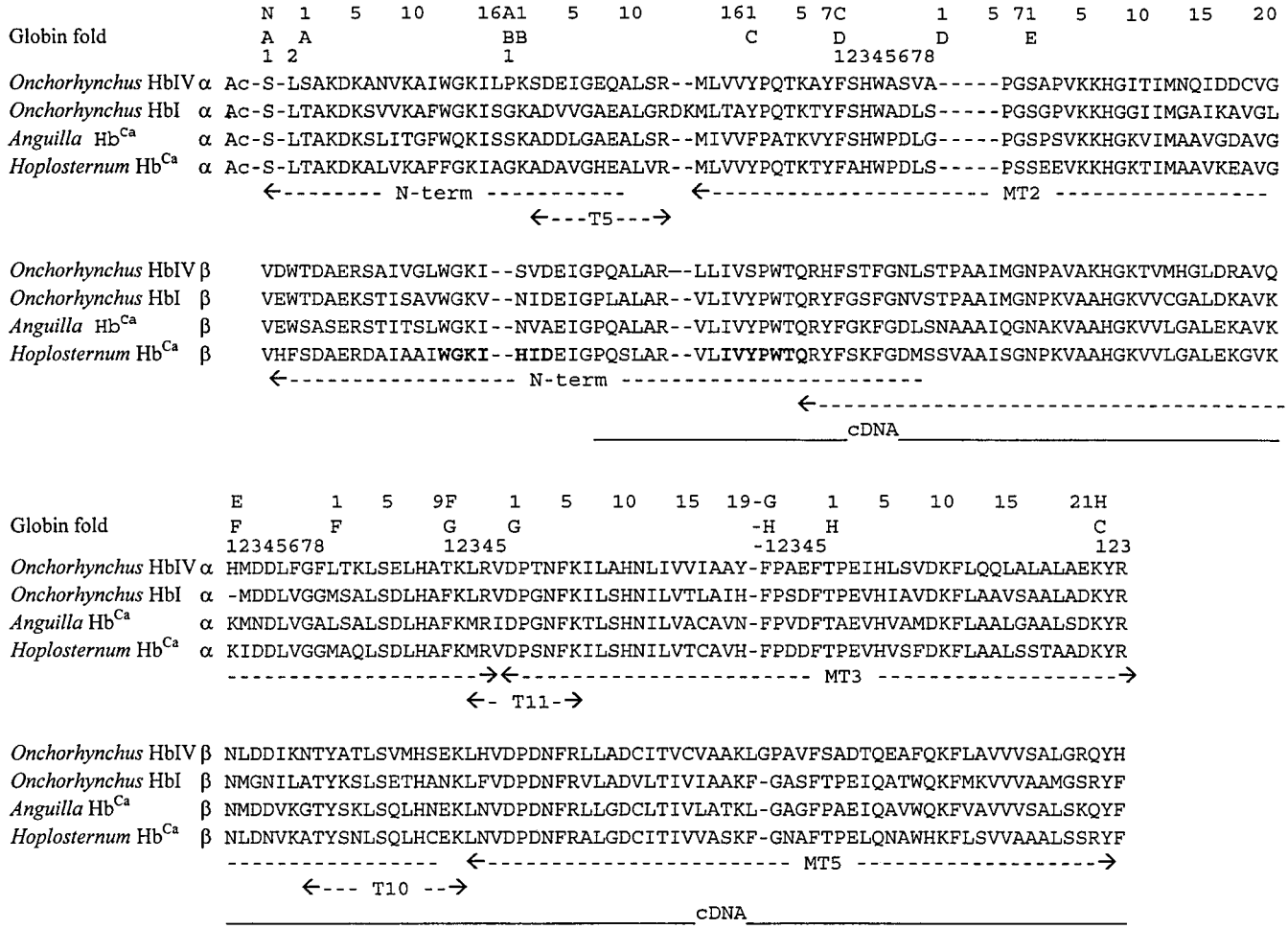

FIG. 11. **Alignment of the amino acid sequences of α and β chains of *Hoplosternum* Hb^{Ca} (Swiss-Prot data base accession numbers P82315 and P82316, respectively) with those of eel (*A. anguilla*) cathodic Hb^{Ca} (accession numbers P80726 and P80727, respectively) and trout (*O. mykiss*) anodic HbIV (accession numbers P14527 and P02141) and cathodic HbI (accession numbers P02019 and P02142).**

His-NA2(β2) in Hb^{Ca} appears to impart no selective advantage for DPG binding, given that Hb^{Ca}, as does Hb^{An}, exhibits markedly lower sensitivities to DPG than to ATP and GTP (Fig. 6).

In view of the large phosphate effects in *Hoplosternum* Hb^{Ca}, the presence of uncharged Ser at H21(β143), compared with His in human Hb and Arg or Lys in other fish Hbs, is unexpected and calls for reconsideration of the importance of individual phosphate-binding sites. Moreover, Ser-H21(β143) also occurs in trout HbI and human fetal Hb that have no and small phosphate effects, respectively. These findings suggest minor significance of H21(β143) for phosphate interaction or that the Glu→His-NA2(β2) exchange in Hb^{Ca} compensates for absence of phosphate binding at this site. A recent NMR study of mutant recombinant Hbs (44) similarly indicates that H21(β143) is not essential for DPG binding in the neutral pH range.

The progressively increasing effects of DPG, ATP, and GTP on O_2 affinity of *Hoplosternum* Hbs (Fig. 6) contrast with human Hb that exhibits similar sensitivities to these effectors (51) and similar binding constants for ATP and DPG (35). In life, however, NTP effects may be drastically reduced as a result of complex formation with divalent cations, since the ATP-Mg^{2+} stability constant exceeds the DPG-Mg^{2+} constants by an order of magnitude (52, 53).

The maximal slope of log P_{50} *versus* log[DPG] curve (Fig. 6) is consistent with a 1:1 (DPG/Hb tetramer) stoichiometry found in human and other mammalian Hbs (34). The τ values exceeding 0.25 observed with IHP and NTP (Fig. 6) could result from binding of these effectors at additional sites. In dromedary Hb, the pattern of Cl^- and phosphate binding similarly indicates the presence of two polyanion sites per tetramer in deoxy and oxygenated Hb, one of which becomes stronger and the other weaker, in terms of affinity, as a result of oxygenation of the molecule (31).

The greater effects of phosphates on O_2 affinity of Hb^{Ca} than Hb^{An} in *Hoplosternum* indicate a dominant role of Hb^{Ca} in adapting blood O_2 affinity to variations under the environmental conditions. In the armored catfish *Hypostomus* and *Pterygoplichthys* hypoxic exposure induces (gut) air breathing and lowers ATP and GTP levels that may increase blood O_2 affinity and exploitation of the O_2 reserves during submersion (54, 55).

Chloride Effects—In human Hb, Cl^- may act either by neutralizing the positive charges in the central cavity without binding to specific residues (56) or bind at specific sites (57). Two major sites generally considered to be implicated in chloride binding in human Hb are Val-NA1(αl) that interacts with Ser-H14(α131) and Lys-EF6(β82) that interacts with Val-NA1(βl) (*cf.* Ref. 43). The τ values for *Hoplosternum* Hbs A and C (0.22) and human Hb (0.48) (Fig. 5) indicate oxygenation-linked binding of 1 and 2 chloride ions, respectively, per tetramer, which accords with acetylation of Val-NA1(αl) in *Hoplosternum* Hb^{Ca} (Fig. 11).

The unexpected increase in O_2 affinity induced in *Hoplosternum* Hb^{An} by 0.1 M Cl^- at pH >7.5 (Fig. 3) may result from Cl^- binding to the R state. It agrees with the observation that in the presence of Cl^-, low DPG and ATP levels raise O_2 affinity of Hb^{An} at pH 7.5 (Fig. 6*D*). Human Hb similarly provides

evidence for Cl^- binding in the oxygenated state (58). The lesser effects of ATP + Cl^- than of ATP in both Hb components (Fig. 3) suggest that Cl^- ions block binding of the phosphate effector at common binding sites.

Band 3 Peptide Effects—The effect of the synthetic trout cd-B3-peptide on the O_2 affinity of *Hoplosternum* Hb^{Ca} provides the first evidence for functionally significant interaction between fish Hb and band 3 proteins, suggesting a possible transducer role for *Hoplosternum* Hb^{Ca} in regulating cellular processes in an oxygen-dependent manner. Band 3 proteins are responsible for HCO_3^-/Cl^- exchange across the red cell membranes, and Hb and glycolytic enzymes (such as aldolase, phosphofructokinase, glyceraldehyde-3-phosphate dehydrogenase, and lactate dehydrogenase) compete for binding to their cytoplasmic domains (16, 59, 60). Thus high O_2 availability releases Hb from the cd-B3 protein that thus become available for inhibiting glycolytic activity and controlling red cell volume via cAMP-dependent NaCl uptake (61).

Why does trout cd-B3 undergo oxygenation-linked binding with *Hoplosternum* HbC and human Hb but not with trout Hbs? We suggest that this is due to the presence of positively charged His at NA2(β2) in *Hoplosternum* Hb^{Ca} and human Hb, given that the lack of effect on trout HbIV may result from repulsion between the peptide and Asp at NA2(β2) (17).

Allosteric Transitions—The allosteric mechanisms controlling O_2 affinity and its dependence on allosteric effectors in Hb^{Ca} are illustrated by the parameters of the MWC model (Table I). At pH 7.5 the K_T:K_R ratio for Hb^{Ca} indicates a 22-fold increase in O_2 affinity between fully deoxy and fully oxygenated Hb, compared with a 35-fold augmentation in human Hb at pH 7.4 (62). Phosphates decrease K_T without significantly changing K_R, thereby increasing ΔG (Fig. 6, Table I). As in eel (14), the reverse Bohr effect in *Hoplosternum* Hb^{Ca} is associated with an increase in K_T and resultant decrease in ΔG with falling pH (Table I). These effects are opposite those in human and other anodic Hbs with normal Bohr effects and suggest that increased bond energies constrain the molecules in the deoxy conformation as pH increases, in contrast to human Hb where additional bonds are formed at low pH (14, 63). The increase in deoxy state bond energies between pH 7.0 and 8.0 (calculated from $\Delta G_T = RT \cdot \ln (K_T^7/K_T^8)$) is 1.9 kJ·mol^{-1}. Analogously, increases in deoxy bond energies imparted in the presence of DPG, ATP, GTP, and IHP at pH 7.5 (estimated as $RT \cdot \ln(K_T^P/K_T^{str})$) are 1.46, 1.35, 2.21, and 2.91 kJ·mol^{-1}, respectively, at phosphate/Hb 2.5, 2.19, 3.16, 3.98, and 4.19 kJ·mol^{-1}, respectively, at phosphate/Hb ~28. These values are low compared with the stabilization energy of internal hydrogen bonds (12 kJ·mol^{-1}) (64) illustrating that small bond energy differences may account for large differences in the effects of individual heterotropic phosphate effectors.

Acknowledgment—We thank Hans Malte (Aarhus) for valuable advice with curve fitting.

REFERENCES

1. Weber, R. E. (1990) *Comp. Physiol.* **6,** 58–75
2. Nikinmaa, M., and Soivio, A. (1982) *J. Exp. Zool.* **219,** 173–178
3. Wood, S. C., and Johansen, K. (1972) *Nat. New Biol.* **237,** 278–279
4. Weber, R. E., and Jensen, F. B. (1988) *Annu. Rev. Physiol.* **50,** 161–179
5. Weber, R. E. (1982) in *Exogenous and Endogenous Influences on Metabolic and Neural Control* (Addink, A. D. F., and Spronk, N., eds) Vol. 1, pp. 87–102, Pergamon Press Ltd., Oxford
6. Nikinmaa, M., and Salama, A. (1998) in *Fish Physiology* (Perry, S. F., and Tufts, B. L., eds) Vol. 17, pp. 141–184, Academic Press, San Diego
7. Powers, D. A. (1972) *Science* **177,** 360–362
8. Nonnotte, G., Maxime, V., Truchot, J. P., Williot, P., and Peyraud, C. (1993) *Respir. Physiol.* **91,** 71–82
9. Pelster, B., and Weber, R. E. (1990) *J. Exp. Biol.* **149,** 425–437
10. Brunori, M., Falcioni, G., Fortuna, G., and Giardina, B. (1975) *Arch. Biochem. Biophys.* **168,** 512–519
11. Weber, R. E., Wood, S. C., and Lomholt, J. P. (1976) *J. Exp. Biol.* **65,** 333–345
12. Weber, R. E., Lykkeboe, G., and Johansen, K. (1976) *J. Exp. Biol.* **64,** 75–88
13. Fago, A., Carratore, V., di Prisco, G., Feuerlein, R. J., Sottrup-Jensen, L., and Weber, R. E. (1995) *J. Biol. Chem.* **270,** 18897–18902
14. Feuerlein, R. J., and Weber, R. E. (1996) *J. Comp. Physiol.* **165,** 597–606
15. Walder, J. A., Chatterjee, R., Steck, T. L., Low, P. S., Musso, G. F., Kaiser, E. T., Rogers, P. H., and Arnone, A. (1984) *J. Biol. Chem.* **259,** 10238–10246
16. Messana, I., Orlando, M., Cassiano, L., Pennacchietti, L., Zuppi, C., Castagnola, M., and Giardina, B. (1996) *FEBS Lett.* **390,** 25–28
17. Jensen, F. B., Jakobsen, M. H., and Weber, R. E. (1998) *J. Exp. Biol.* **201,** 2685–2690
18. Carter, G. S., and Beadle, L. C. (1931) *J. Linn. Soc. (Lond.)* **37,** 327–368
19. Val, A. L. (1993) in *The Vertebrate Gas Transport Cascade. Adaptations to Environment and Mode of Life* (Bicudo, J. E. P. W., ed) pp. 43–53, CRC Press Inc., Boca Raton, FL
20. Affonso, E. G. (1990) *Estudo Sazonal De Caracteristicas Respiratorias Do Sanque De Hoplosternum Littorale (Siluriformes, Calichthyidae) da ilha da Marchantaria, Amazonas*, Ph.D. thesis, INPA, Manaus, Brazil
21. Garlick, R. L., Bunn, H. F., Fyhn, H. J., Fyhn, U. E. H., Martin, J. P., Noble, R. W., and Powers, D. (1979) *Comp. Biochem. Physiol.* **62,** 219–226
22. Monod, J., Wyman, J., and Changeux, J.-P. (1965) *J. Mol. Biol.* **12,** 88–118
23. Weber, R. E., Jensen, F. B., and Cox, R. P. (1987) *J. Comp. Physiol.* **157,** 145–152
24. Weber, R. E. (1992) *J. Appl. Physiol.* **72,** 1611–1615
25. Weber, R. E. (1981) *Nature* **292,** 386–387
26. Hübner, S., Michel, F., Rudloff, V., Appelhans, H., and Hubner, S. (1992) *Biochem. J.* **285,** 17–23
27. Weber, R. E., Malte, H., Braswell, E. H., Oliver, R. W. A., Green, B. N., Sharma, P. K., Kuchumov, A., and Vinogradov, S. N. (1995) *J. Mol. Biol.* **251,** 703–720
28. Rossi-Fanelli, A., Antonini, E., and Caputo, A. (1958) *Biochim. Biophys. Acta* **30,** 608–615
29. Allen, G. (1989) in *Laboratory Techniques in Biochemistry and Molecular Biology*, (Burton, R. H., and Knippenberg, P. H., eds) Vol. 9, pp. 1–424, Elsevier/North-Holland Biomedical Press, Amsterdam
30. Dewilde, S., Blaxter, M., Van Hauwaert, M. L., Vanfleteren, J., Esmans, E. L., Marden, M., Griffon, N., and Moens, L. (1996) *J. Biol. Chem.* **271,** 19865–19870
31. Amiconi, G., Bertollini, A., Bellelli, A., Coletta, M., Condò, S. G., and Brunori, M. (1985) *Eur. J. Biochem.* **150,** 387–393
32. Giardina, B., Brix, O., Colosimo, A., Petruzzelli, R., Cerroni, L., and Condò, S. G. (1990) *Eur. J. Biochem.* **194,** 61–65
33. Giardina, B., Brix, O., Clementi, M. E., Scatena, R., Nicoletti, B., Cicchetti, R., Argentin, G., and Condò, S. G. (1990) *Biochem. J.* **266,** 897–900
34. Bårdgard, A. J., Strand, I., Nuutinen, M., Jul, E., and Brix, O. (1997) *Comp. Biochem. Physiol. A Comp. Physiol.* **117,** 367–373
35. Imai, K. (1982) *Allosteric Effects in Haemoglobin,* pp. 1–275, Cambridge University Press, Cambridge
36. Chien, J. C. W., and Mayo, K. H. (1980) *J. Biol. Chem.* **255,** 9790–9799
37. Imai, K., and Yonetani, T. (1975) *J. Biol. Chem.* **250,** 2227–2231
38. Barra, D., Petruzzelli, R., Bossa, F., and Brunori, M. (1983) *Biochim. Biophys. Acta* **742,** 72–77
39. Fago, A., D'Avino, R., and di Prisco, G. (1992) *Eur. J. Biochem.* **210,** 963–970
40. Weber, R. E., and Wood, S. C. (1979) *Comp. Biochem. Physiol.* **62,** 179–183
41. Martin, J. P., Bonaventura, J., Brunori, M., Fyhn, H. J., Fyhn, U. E. H., Garlick, R. L., Powers, D. A., and Wilson, M. T. (1979) *Comp. Biochem. Physiol.* **62,** 155–162
42. Shih, D. T., Luisi, B. F., Miyazaki, G., Perutz, M. F., and Nagai, K. (1993) *J. Mol. Biol.* **230,** 1291–1296
43. Riggs, A. F. (1988) *Annu. Rev. Physiol.* **50,** 181–204
44. Fang, T. Y., Zou, M., Simplaceanu, V., Ho, N. T., and Ho, C. (1999) *Biochemistry* **38,** 13423–13432
45. Fago, A., Bendixen, E., Malte, H., and Weber, R. E. (1997) *J. Biol. Chem.* **272,** 15628–15635
46. Perutz, M. F., and Brunori, M. (1982) *Nature* **299,** 421–426
47. Gronenborn, A. M., Clore, G. M., Brunori, M., Giardina, B., Falcioni, G., and Perutz, M. F. (1984) *J. Mol. Biol.* **178,** 731–742
48. Kleinschmidt, T., and Sgouros, J. G. (1987) *Biol. Chem. Hoppe-Seyler* **368,** 579–615
49. Isaacks, R. E., Kim, H. D., and Harkness, D. R. (1978) *Can. J. Zool.* **56,** 1014–1016
50. Weber, R. E., Wells, R. M. G., and Rossetti, J. E. (1983) *J. Exp. Biol.* **103,** 109–120
51. Chanutin, A., and Curnish, R. R. (1967) *Arch. Biochem. Biophys.* **121,** 96–102
52. Bunn, H. F., Ransil, B. J., and Chao, A. (1971) *J. Biol. Chem.* **246,** 5273–5279
53. Weber, R. E., and Lykkeboe, G. (1978) *J. Comp. Physiol.* **128,** 127–137
54. Weber, R. E., Wood, S. C., and Davis, B. J. (1979) *Comp. Biochem. Physiol.* **62,** 125–129
55. Val, A. L., Almeida-Val, V. M. F., and Affonso, E. G. (1990) *Comp. Biochem. Physiol.* **97,** 435–440
56. Perutz, M. F., Shih, D. T., and Williamson, D. (1994) *J. Mol. Biol.* **239,** 555–560
57. Fronticelli, C., Pechik, I., Brinigar, W. S., Kowalczyk, J., and Gilliland, G. L. (1994) *J. Biol. Chem.* **269,** 23965–23969
58. Rollema, H. S., de Bruin, S. H., Janssen, L. H. M., and Van Os, G. A. J. (1975) *J. Biol. Chem.* **250,** 1333–1339
59. Low, P. S. (1986) *Biochim. Biophys. Acta* **864,** 145–167
60. Giardina, B., Messana, I., Scatena, R., and Castagnola, M. (1995) *Crit. Rev. Biochem. Mol. Biol.* **30,** 165–196
61. Motais, R., Garcia Romeu, F., and Borgese, F. (1987) *J. Gen. Physiol.* **90,** 197–207
62. Tyuma, I., Imai, K., and Shimizu, K. (1973) *Biochemistry* **12,** 1491–1498
63. Perutz, M. F. (1970) *Nature* **228,** 726–734
64. Garrett, R. H., and Grisham, C. M. (1995) *Biochemistry*, pp. 1–1100, Saunders College Publishing, Fort Worth, TX
65. Hancock, J. (1828) *Zool. J.* **4,** 240–247

Isohemoglobin Differentiation in the Bimodal-breathing Amazon Catfish *Hoplosternum littorale*

Roy E. Weber, Angela Fago, Adalberto L. Val, Anny Bang, Marie-Louise Van Hauwaert, Sylvia Dewilde, Franck Zal and Luc Moens

J. Biol. Chem. 2000, 275:17297-17305.
doi: 10.1074/jbc.M001209200 originally published online March 27, 2000
